Electronic Supplementary Information

Metal ions induced coordination and cyclization of crownether-based bisindolylmaleimides: different fluorescent response and application in complex logical operations

Qiuqin Huang, Zhengde Liu, Limei Huang, Zhenghuan Lin*, and Qidan Ling

College of Chemistry and Materials Science, Fujian Key Laboratory of Polymer Materials, Fujian Normal University, Fuzhou 350007, Fujian, China.

Email: zhlin@fjnu.edu.cn

Tel.: +86 591 83464353; fax: +86 591 83464353

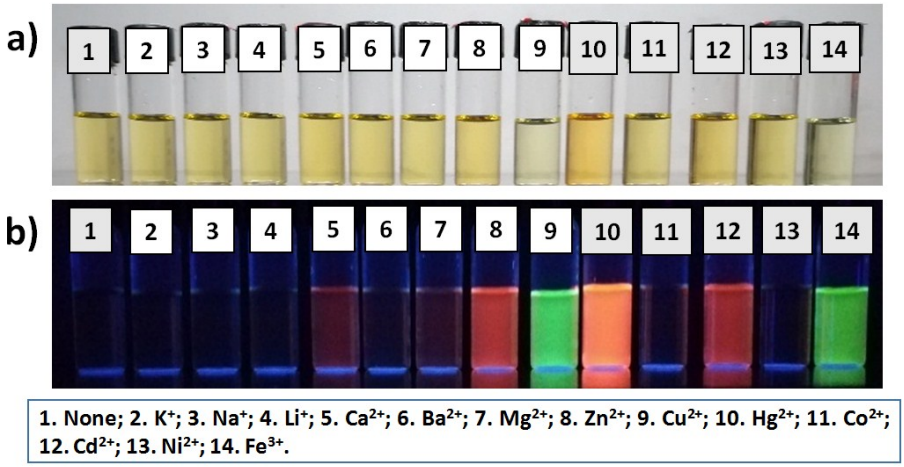

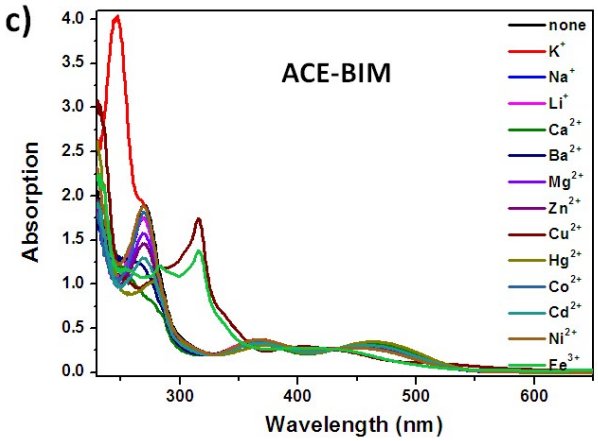

Fig. S1 ACE-BIM (5×10^{-5} M) in CH_3CN upon various metal ions (5 equiv): Photographs under visible light (a) and 365 nm of UV light (b); (c) Absorption spectra.

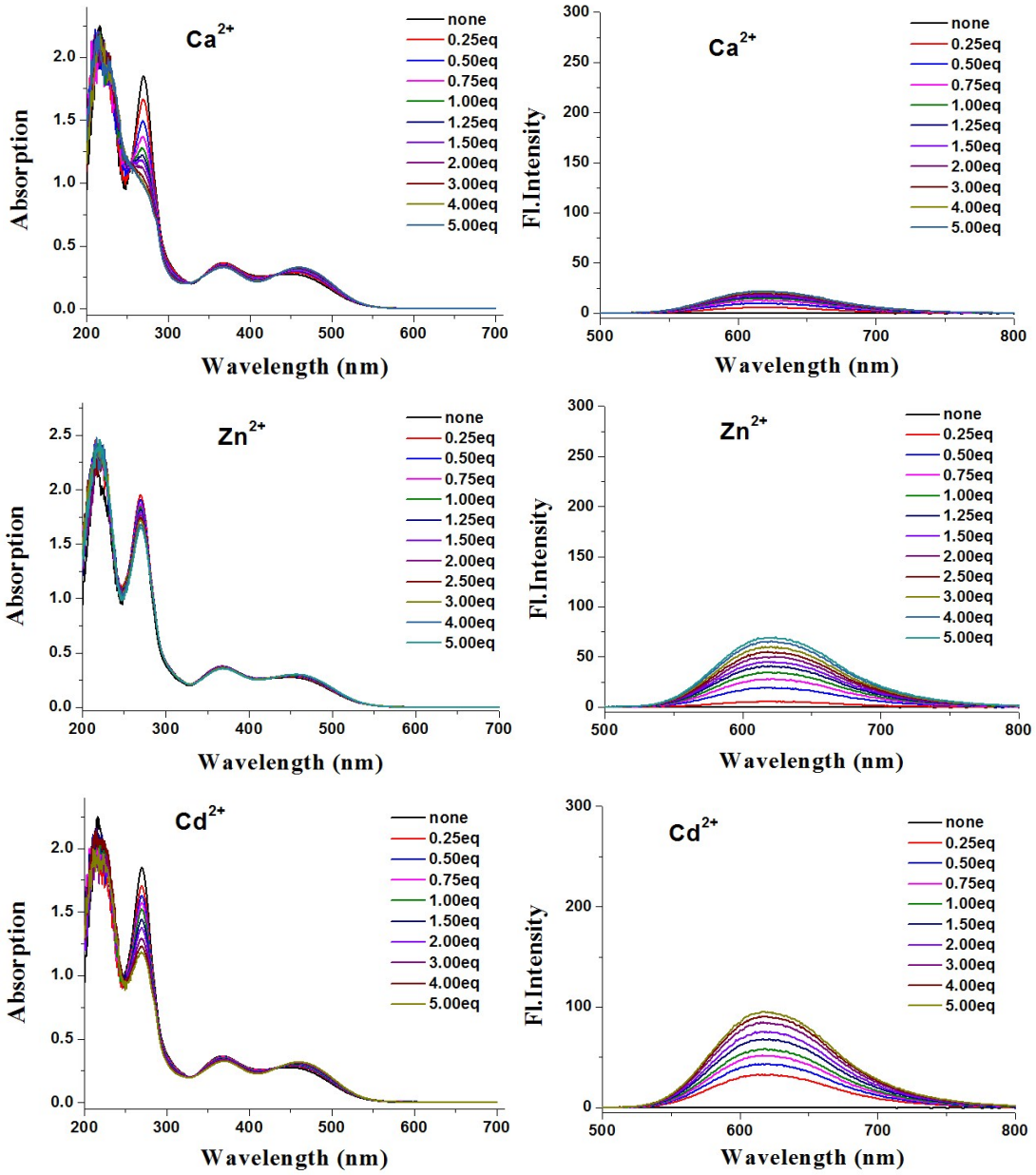

Fig. S2 Abosrption (left) and emission (right) spectra of ACE-BIM (5×10^{-5} M) in CH_3CN upon titration with Ca^{2+}, Zn^{2+} and Cd^{2+}.

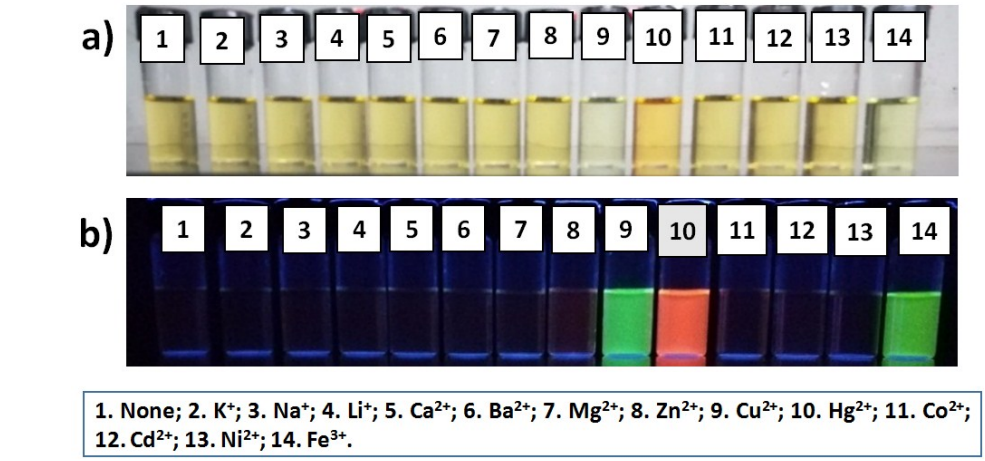

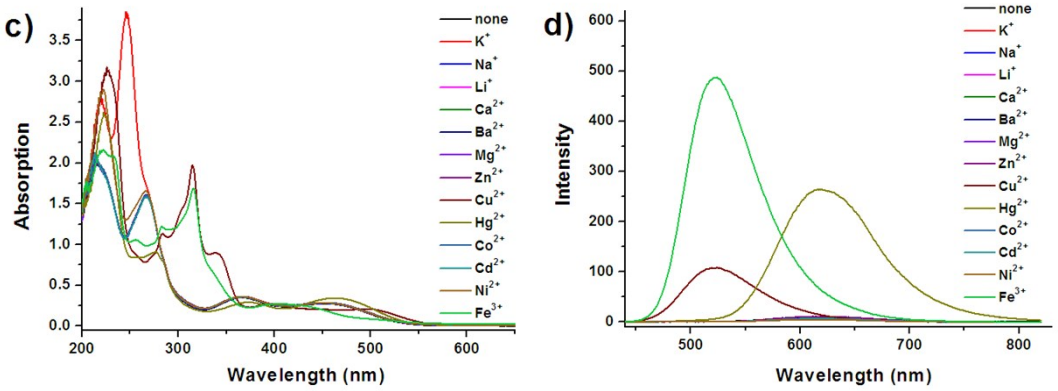

Fig. S3 AB-BIM in CH_3CN (5×10^{-5} M) upon various metal ions (5 equiv): Photographs under visible light (a) and 365 nm of UV light (b); Absorption (c) and emission (d) spectra.

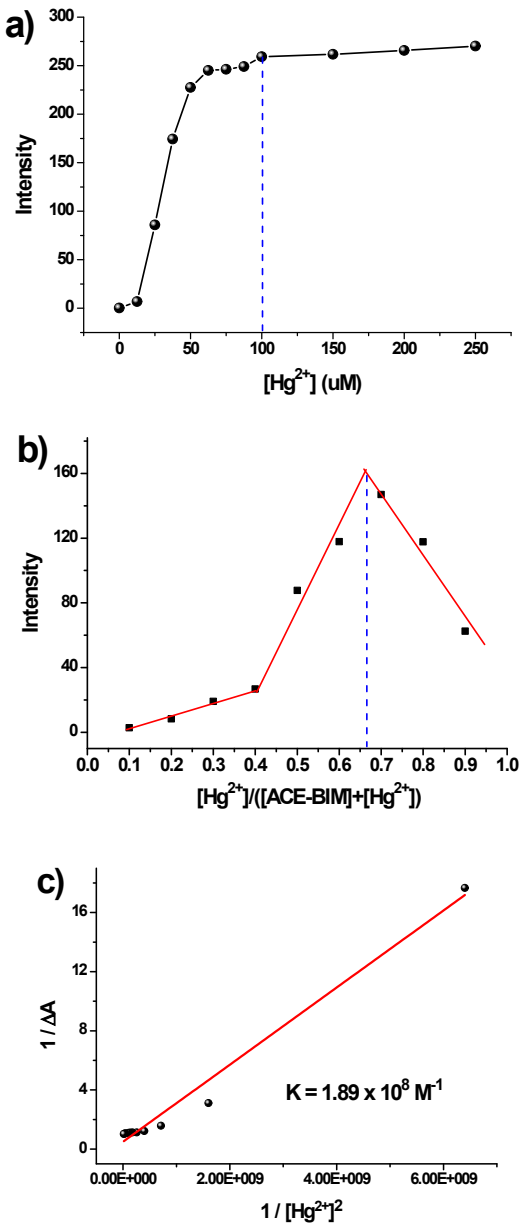

Fig. S4 (a) Changes of emission intensity at 618 nm of ACE-BIM (5×10^{-5} M) in CH_3CN upon titration of Hg^{2+} (λ_{ex} = 425 nm). (b) Job's plots for the complexation of ACE-BIM and Hg^{2+} in CH_3CN constructed by monitoring the fluorenscence intensity at 618 nm. (c) Linear fitting curve of Benesi-Hildebrand for determination of the binding constant *K*.

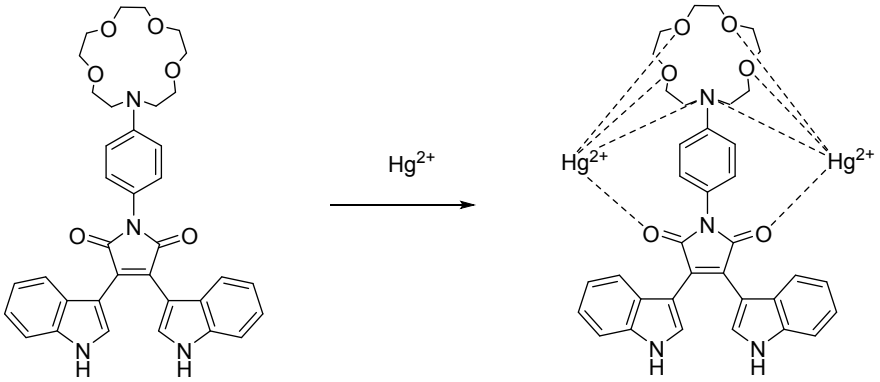

Scheme S1 Possible interaction of ACE-BIM with Hg^{2+} ion.

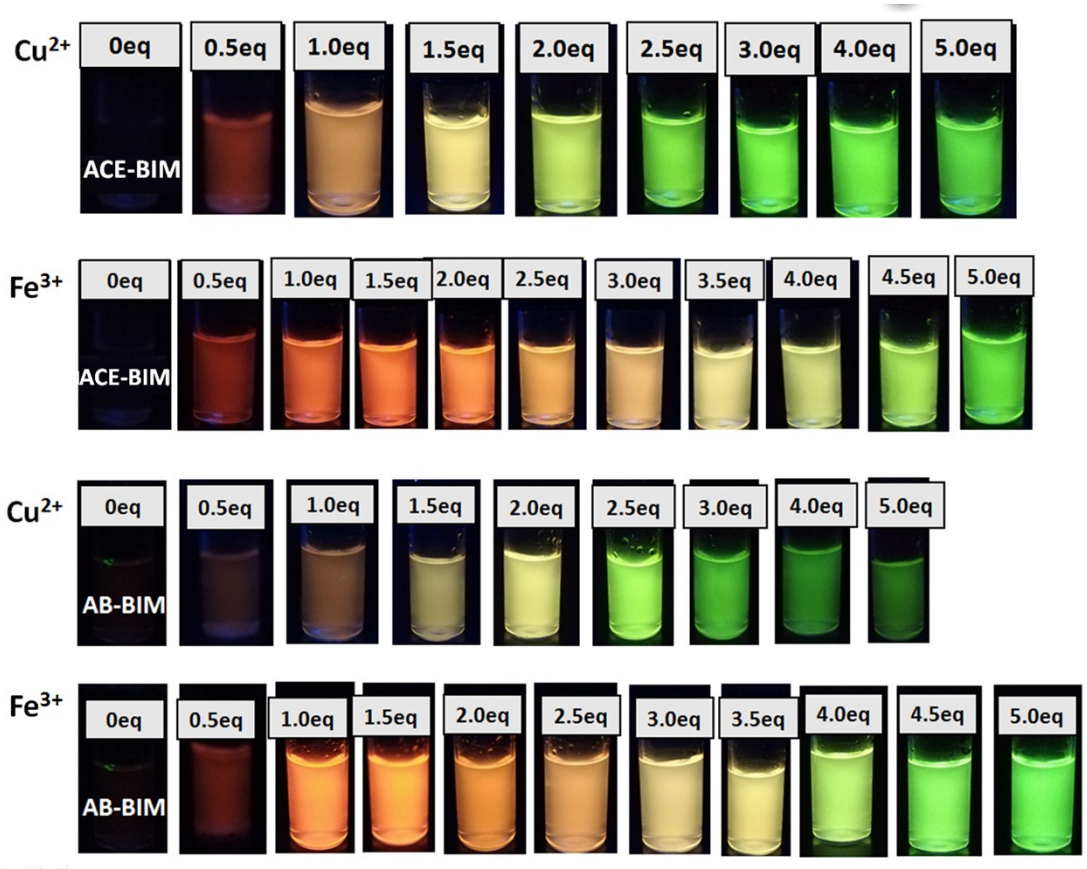

Fig. S5 Photographs of ACE-BIM and AB-BIM in CH_3CN upon titration of Cu^{2+} or Fe^{3+} ion under 365 nm of UV light.

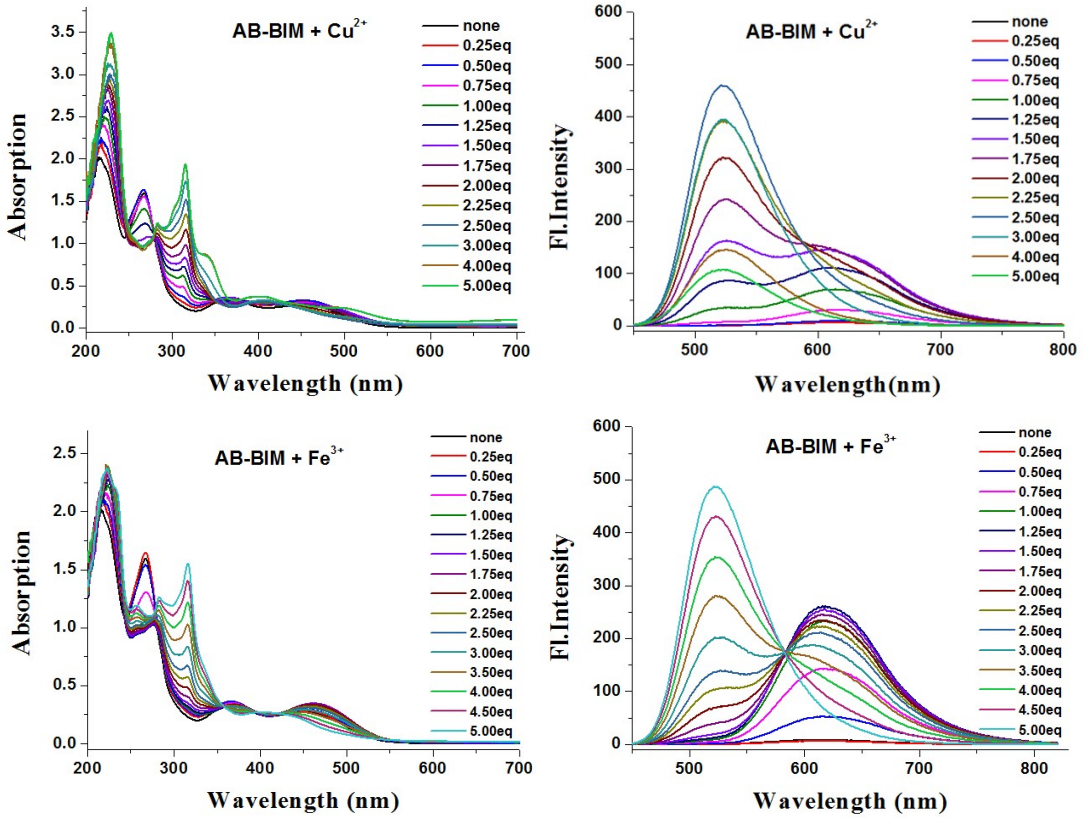

Fig. S6 Absorption (left) and emission (right) spectra of AB-BIM in CH_3CN (5×10^{-5} M) upon titration with Cu^{2+} (upper) and Fe^{3+} (bottom) (λ_{ex} = 425 nm).

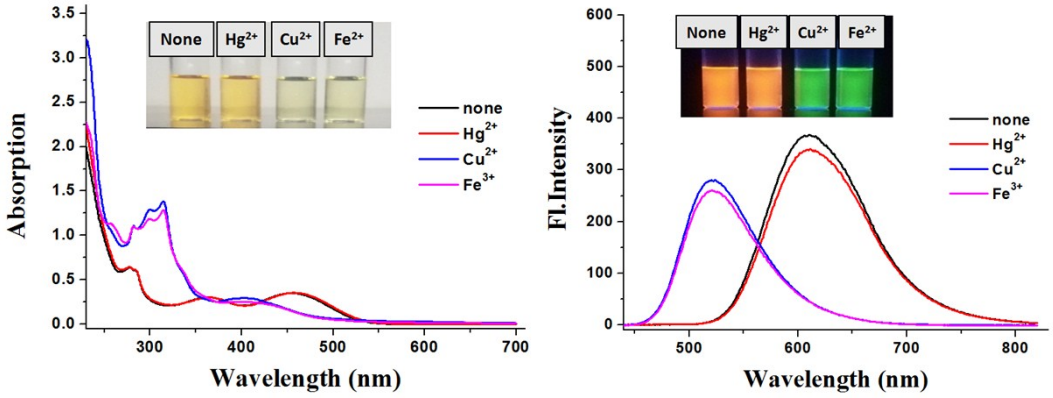

Fig. S7 Absorption (left) and emission (right) spectra of MB-BIM in CH_3CN (5×10^{-5} M) upon 5 equiv of Hg^{2+}, Cu^{2+} and Fe^{3+} ions. Insert: photos of MB-BIM with Hg^{2+}, Cu^{2+} and Fe^{3+} ions under sun light (left) and 365 nm of UV light.

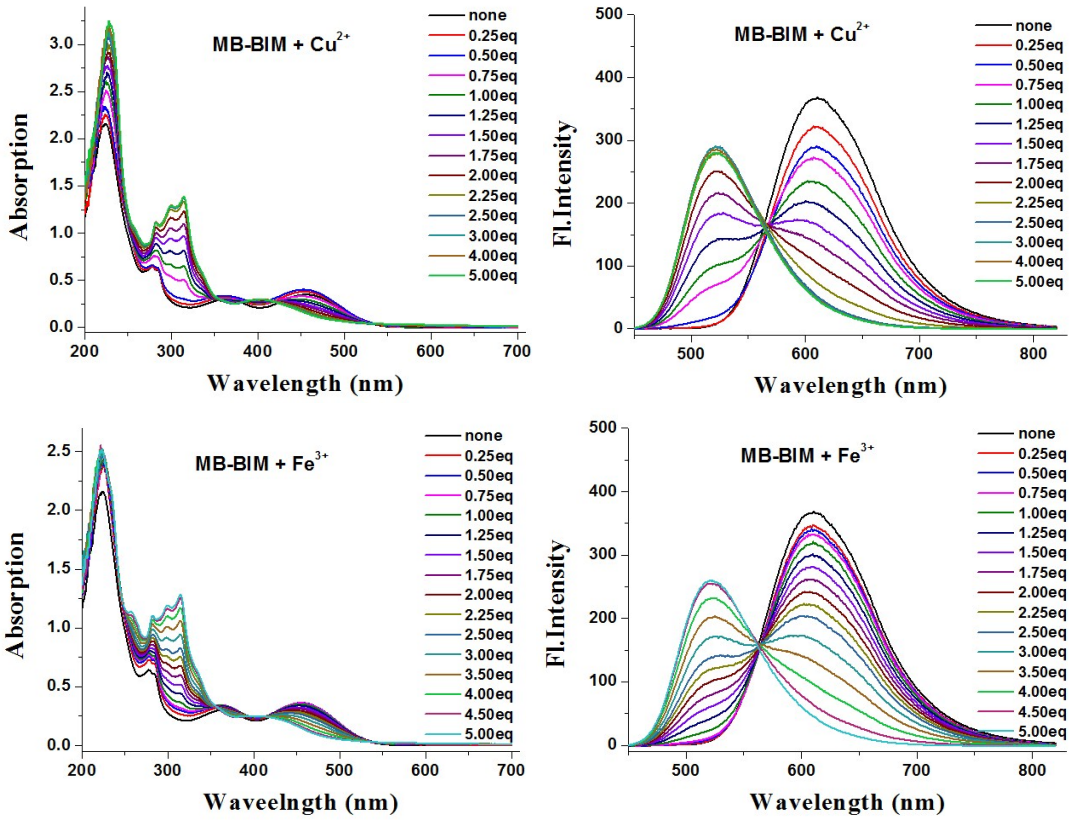

Fig. S8 Absorption (left) and emission (right) spectra of AB-BIM in CH_3CN (5×10^{-5} M) upon titration with Cu^{2+} (upper) and Fe^{3+} (bottom) (λ_{ex} = 425 nm).

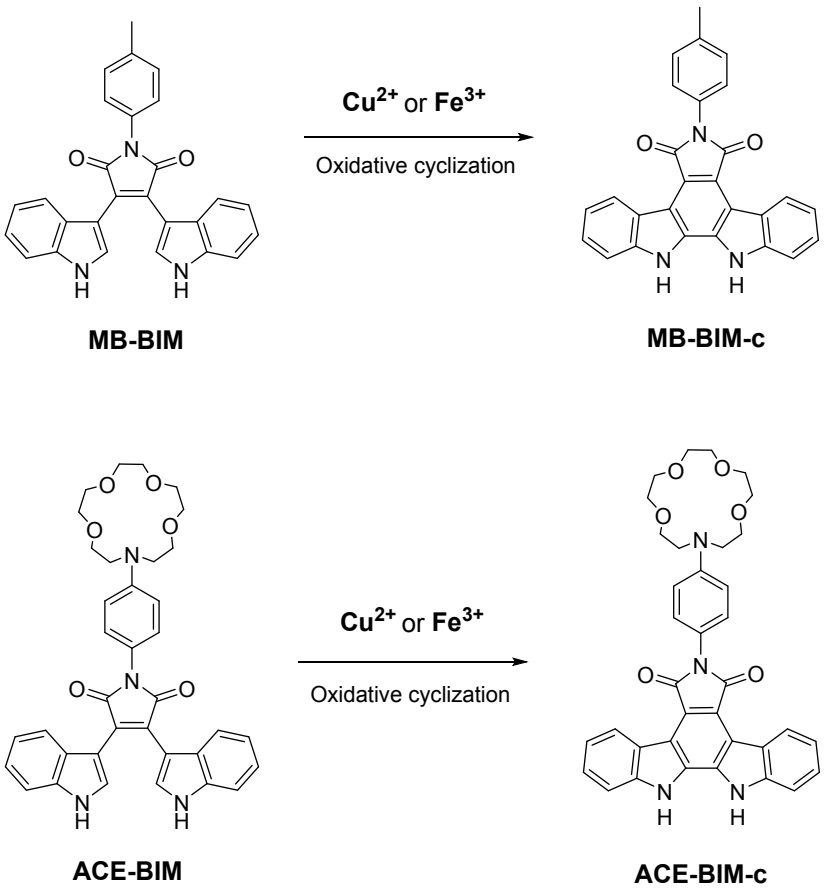

Scheme S2 Oxidative cyclization of MB-BIM and ACE-BIM.

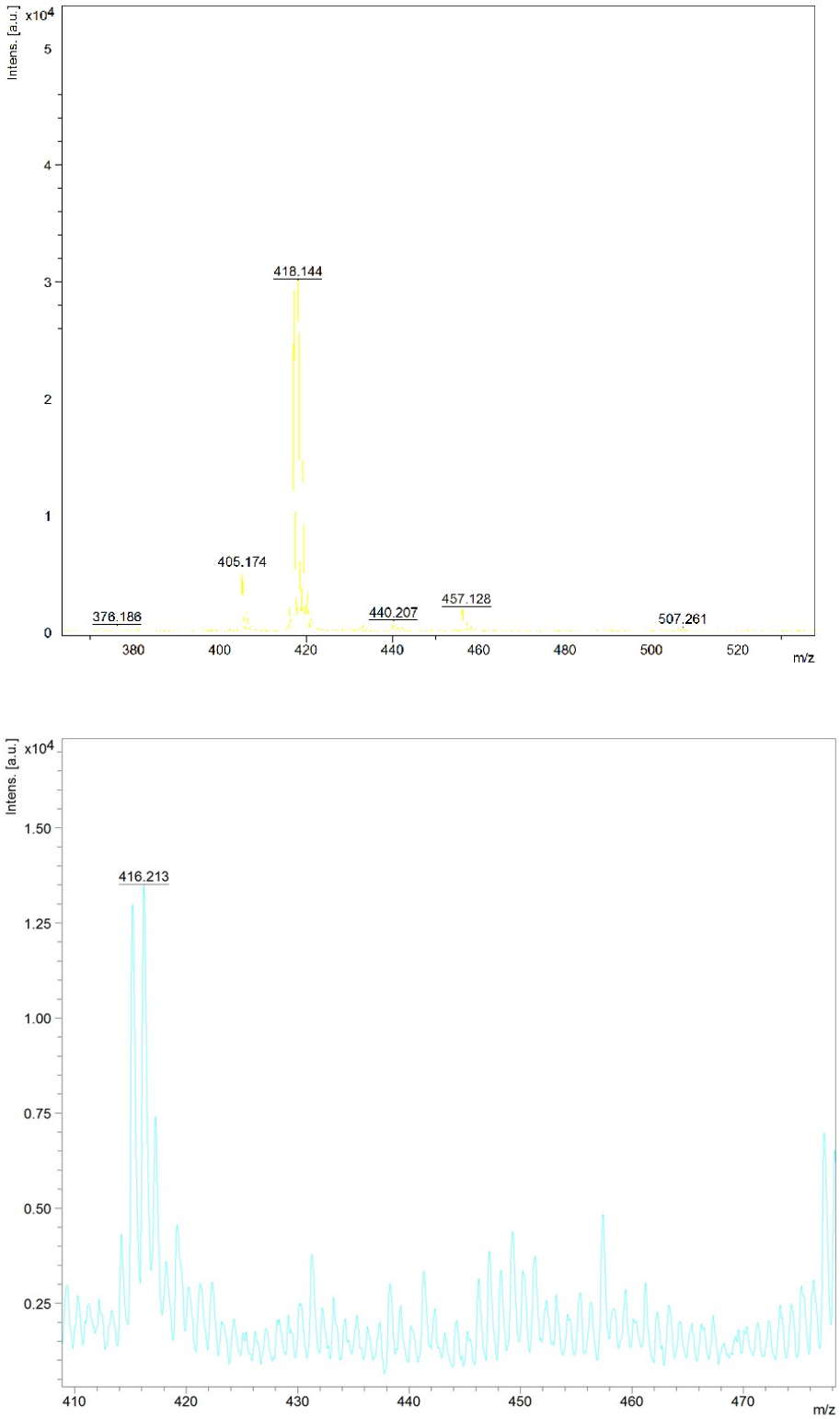

Fig. S9 MALDI-TOF MS of MB-BIM (upper) and MB-BIM-c (bottom).

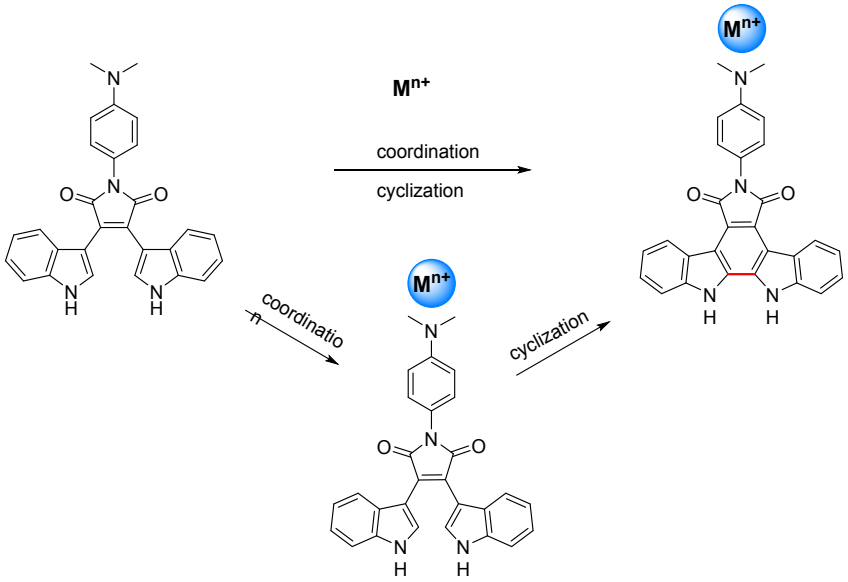

Scheme S3 Possible interaction mechanism of AB-BIM with Cu^{2+} and Fe^{3+} (M^{n+} = Cu^{2+} or Fe^{3+}).

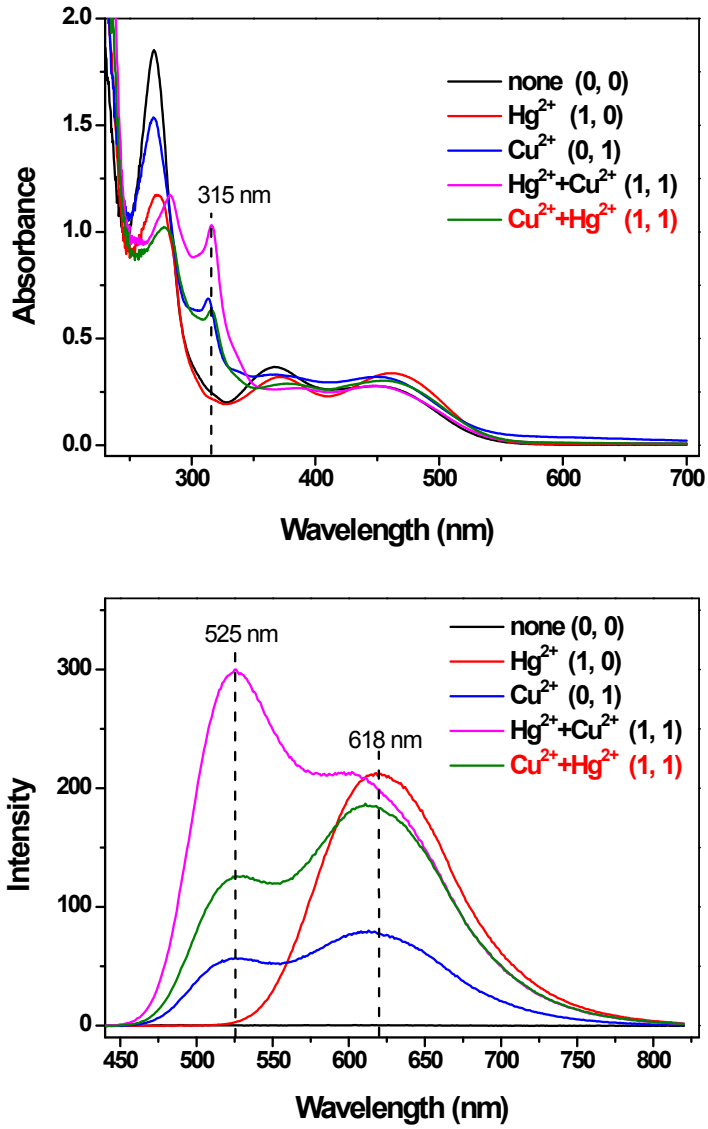

Fig. S10 Absorption (upper) and emission (bottom) spectra of ACE-BIM in CH_3CN (5×10^{-5}M) under different combination conditions of two inputs (1 equiv of Hg^{2+} and Cu^{2+}).

Table S1 Truth table for molecular 2-to-4 decoder base on ACE-BIM with two inputs (1 equiv Hg^{2+} and Cu^{2+}).

In1 (Hg^{2+})	**In2** (Cu^{2+})	$I_{E,618}$	$I_{A,315}$	**O1** (0, 0)	**O2** (0, 1)	**O3** (1, 0)	**O4** (1, 1)
0	0	0	0	1	0	0	0
1	0	1	0	0	1	0	0
0	1	0	1	0	0	1	0
1	1	1	1	0	0	0	1

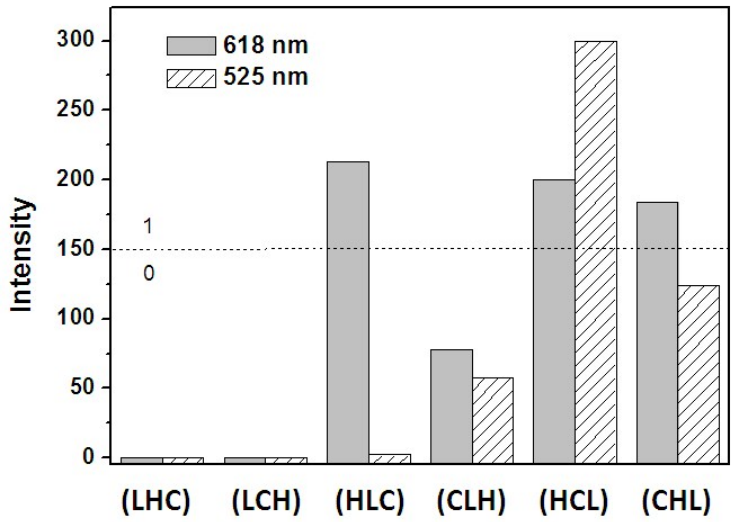

Fig. S11 Outputs ($I_{E,618}$ and $I_{E,525}$) of molecular keypad lock based on ACE-BIM in response to three inputs (H = Hg^{2+}, C = Cu^{2+}, and L = light excitation).

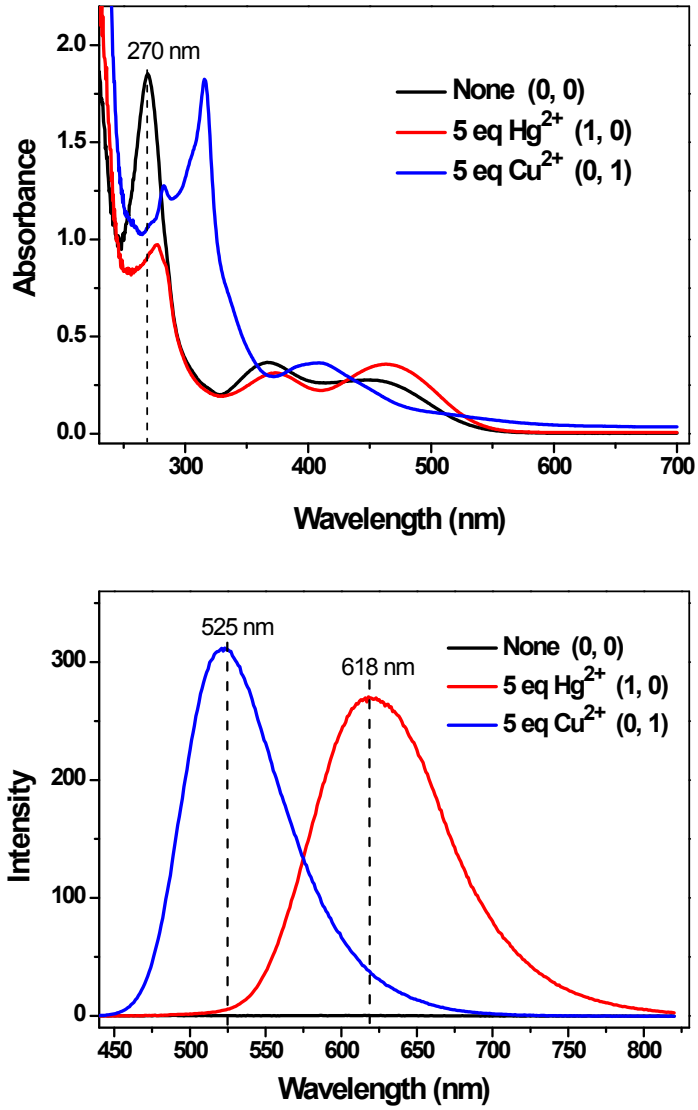

Fig. S12 Absorption (upper) and emission (bottom) spectra of ACE-BIM in CH_3CN (5×10^{-5}M) under different combination conditions of two inputs (5 equiv of Hg^{2+} and Cu^{2+}).

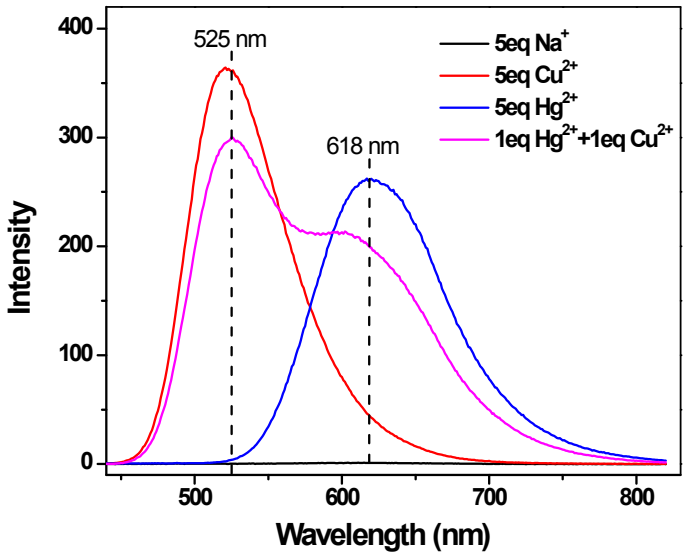

Fig. S13 Emission spectra of ACE-BIM in CH_3CN (5×10^{-5}M) under four different inputs (5 equiv of Na^+, Hg^{2+} and Cu^{2+} and 1 equiv of Hg^{2+}/Cu^{2+}).

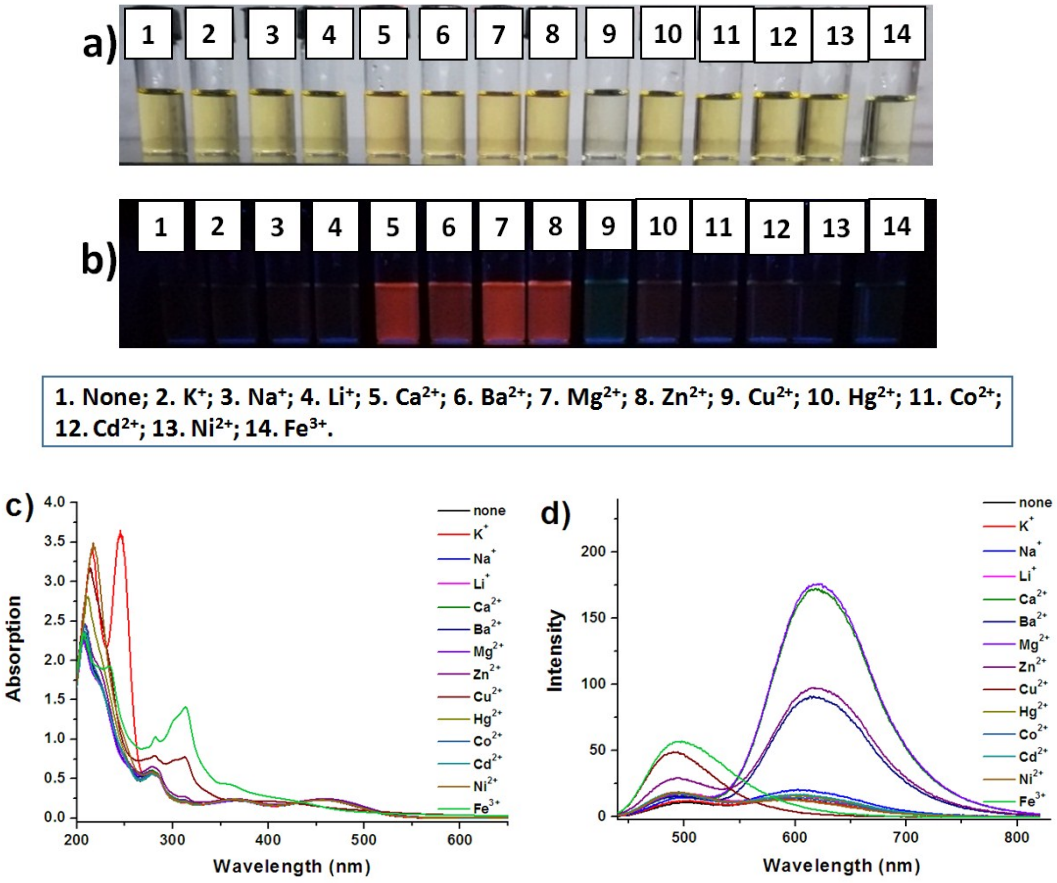

Fig. S14 BCE-BIM in CH_3CN (5×10^{-5} M) upon various metal ions (5 equiv): Photographs under visible light (a) and 365 nm of UV light (b); Absorption (c) and emission (d) spectra (λ_{ex} = 425 nm).

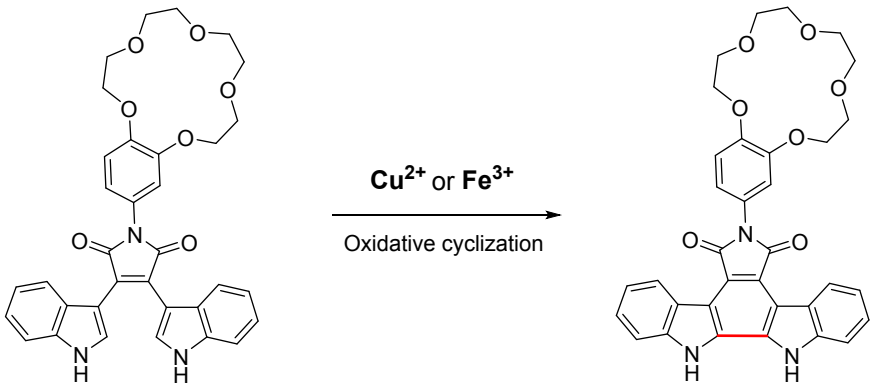

Scheme S4 Oxidative cyclization of BCE-BIM to give BCE-BIM-c.

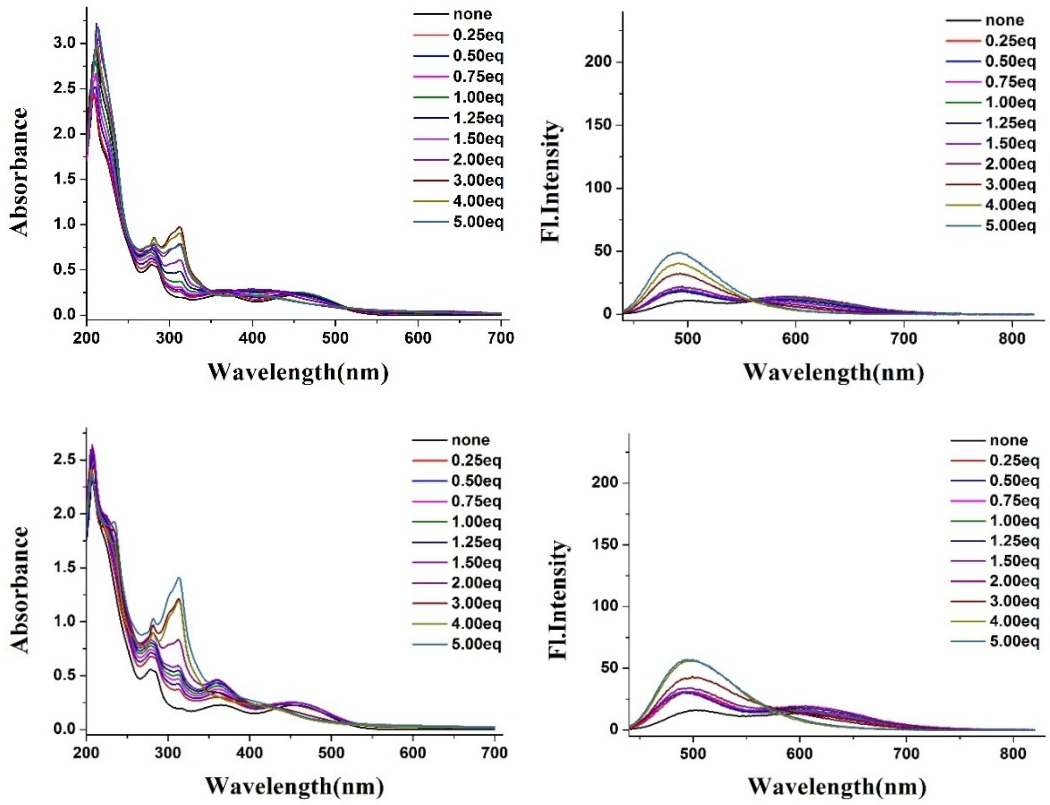

Fig. S15 Absorption (left) and emission (right) spectra of BCE-BIM in CH_3CN (5×10^{-5} M) upon titration with Cu^{2+} (upper) and Fe^{3+} (bottom) (λ_{ex} = 425 nm).

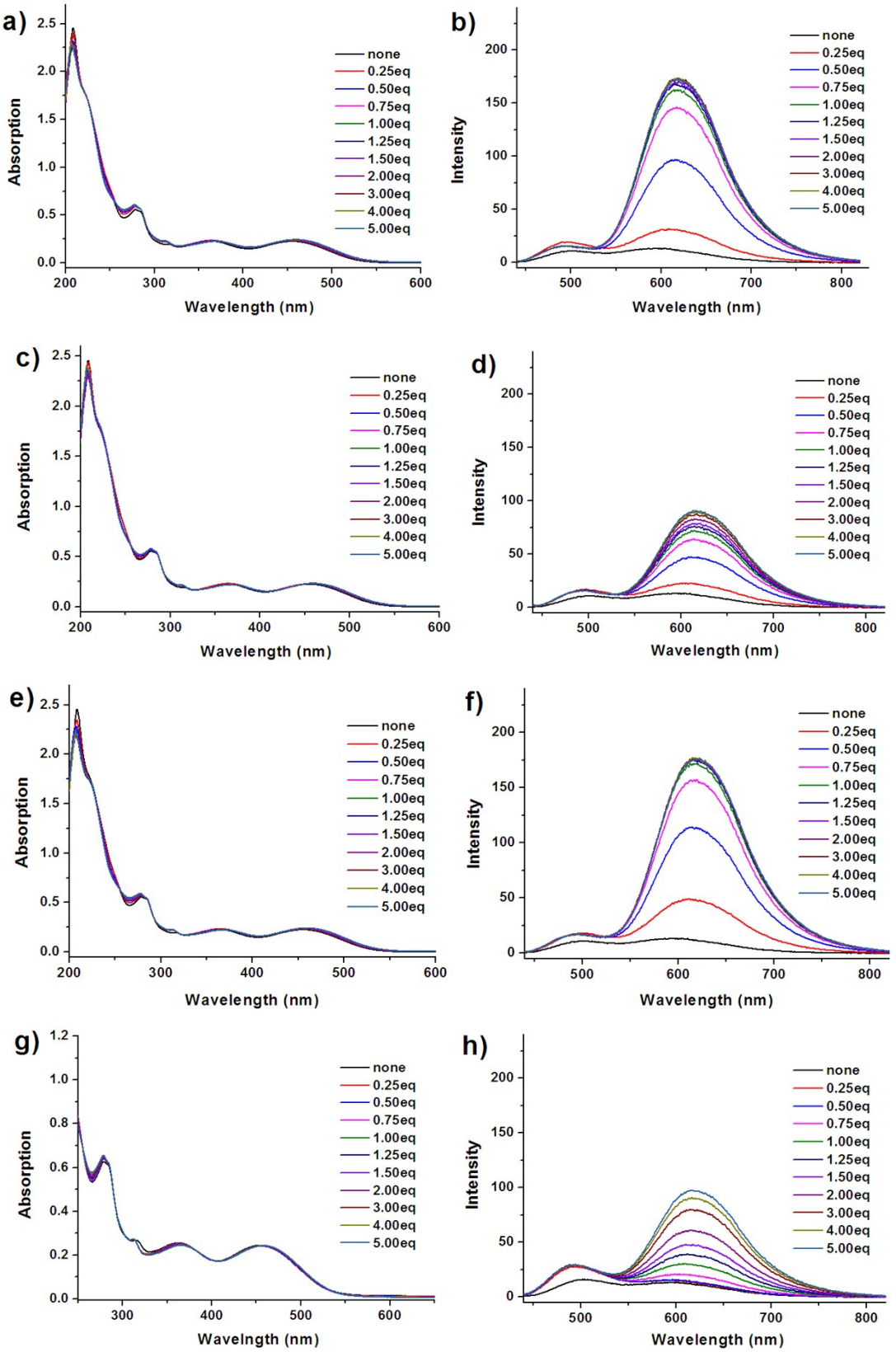

Fig. S16 Absorption (a, c, e, g) and emission (b, d, f, h) spectra of BCE-BIM in CH_3CN (5×10^{-5} M) upon titration with Ca^{2+} (a, b), Ba^{2+} (c, d), Mg^{2+} (e, f) and Zn^{2+} (g, h) (λ_{ex} = 425 nm).

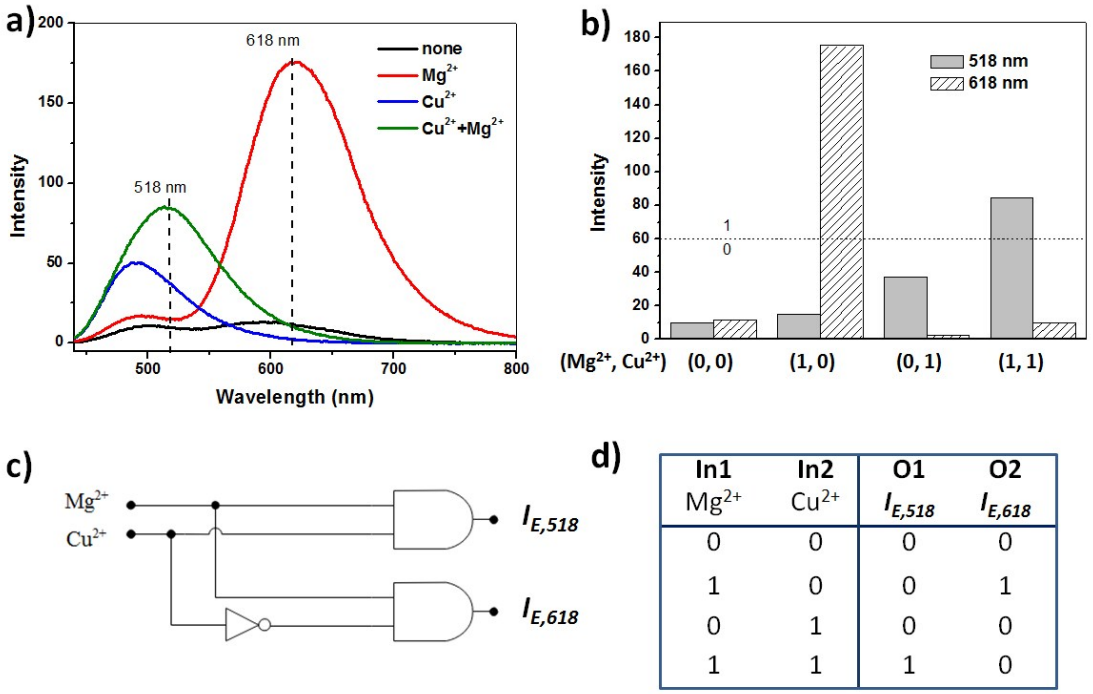

In1 Mg^{2+}	In2 Cu^{2+}	O1 $I_{E,518}$	O2 $I_{E,618}$
0	0	0	0
1	0	0	1
0	1	0	0
1	1	1	0

Fig. S17 Emission spectra (a) and outputs of $I_{E,518}$ and $I_{E,618}$ (b) of BCE-BIM in CH_3CN (5×10^{-5}M) under different combination conditions of two inputs (5 equiv of Mg^{2+} and Cu^{2+}). Circuit symbols (c) and truth table (d) of 1:2 demultiplexer.

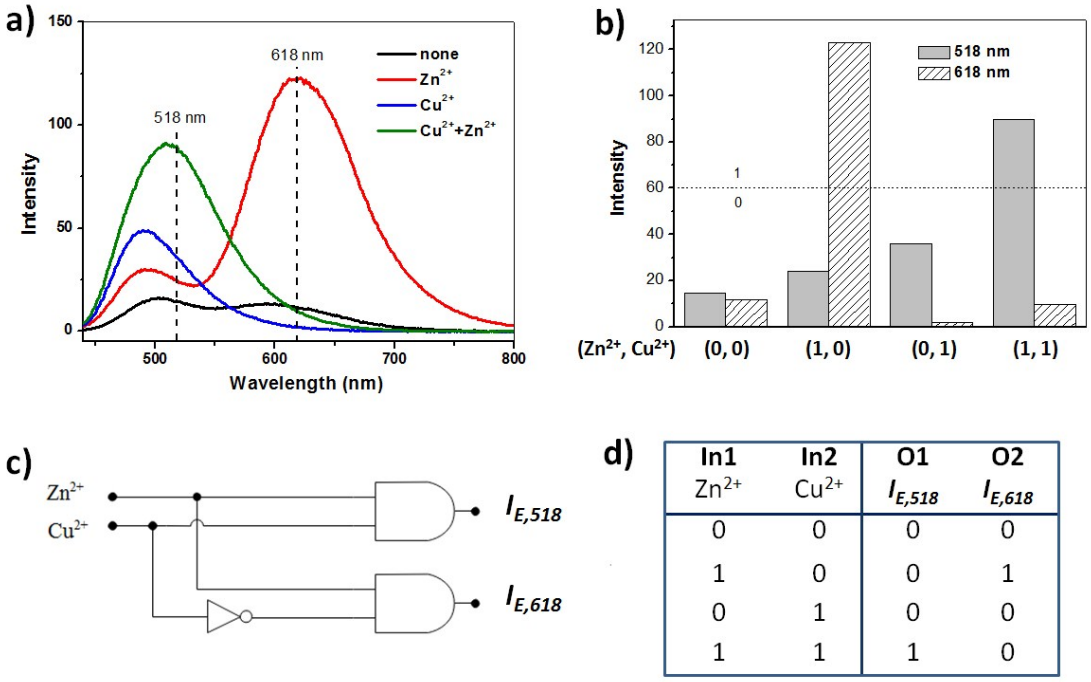

In1 Zn^{2+}	In2 Cu^{2+}	O1 $I_{E,518}$	O2 $I_{E,618}$
0	0	0	0
1	0	0	1
0	1	0	0
1	1	1	0

Fig. S18 Emission spectra (a) and outputs of $I_{E,518}$ and $I_{E,618}$ (b) of BCE-BIM in CH_3CN (5×10^{-5}M) under different combination conditions of two inputs (5 equiv of Zn^{2+} and Cu^{2+}). Circuit symbols (c) and truth table (d) of 1:2 demultiplexer.

Table S2 Truth table for combinatorial logic operations based on BCE-BIM with four-input and two-output (Threshold value of 60).

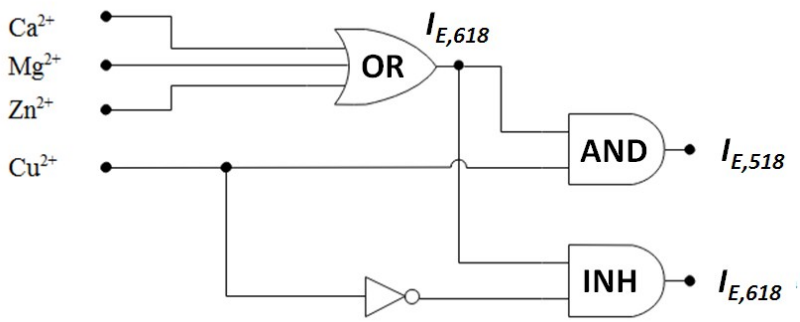

Entry	**In1** (Ca^{2+})	**In2** (Mg^{2+})	**In3** (Zn^{2+})	**In4** (CU^{2+})	**O1** ($I_{E,518}$)	**O2** ($I_{E,618}$)
1	0	0	0	0	0	0
2	1	0	0	0	0	1
3	0	1	0	0	0	1
4	0	0	1	0	0	1
5	0	0	0	1	0	0
6	1	1	0	0	0	1
7	1	0	1	0	0	1
8	1	0	0	1	1	0
9	0	1	1	0	0	1
10	0	1	0	1	1	0
11	0	0	1	1	1	0
12	1	1	1	0	0	1
13	1	1	0	1	1	0
14	1	0	1	1	1	0
15	0	1	1	1	1	0
16	1	1	1	1	1	0

Table S3 Truth table for combinatorial logic operations based on BCE-BIM with four-input and four-output (Threshold value of 35).

Entry	**In1** (Ca^{2+})	**In2** (Mg^{2+})	**In3** (Zn^{2+})	**In4** (CU^{2+})	**O1** ($I_{E,540}$)	**O2** ($I_{E,618}$)	**O3** ($I_{E,560}$)	**O4** ($I_{E,490}$)
1	0	0	0	0	0	0	0	0
2	1	0	0	0	0	1	1	0
3	0	1	0	0	0	1	1	0
4	0	0	1	0	0	1	1	0
5	0	0	0	1	0	0	0	1
6	1	1	0	0	0	1	1	0
7	1	0	1	0	0	1	1	0
8	1	0	0	1	1	0	1	1
9	0	1	1	0	0	1	1	0
10	0	1	0	1	1	0	1	1
11	0	0	1	1	1	0	1	1
12	1	1	1	0	0	1	1	0
13	1	1	0	1	1	0	1	1
14	1	0	1	1	1	0	1	1
15	0	1	1	1	1	0	1	1
16	1	1	1	1	1	0	1	1

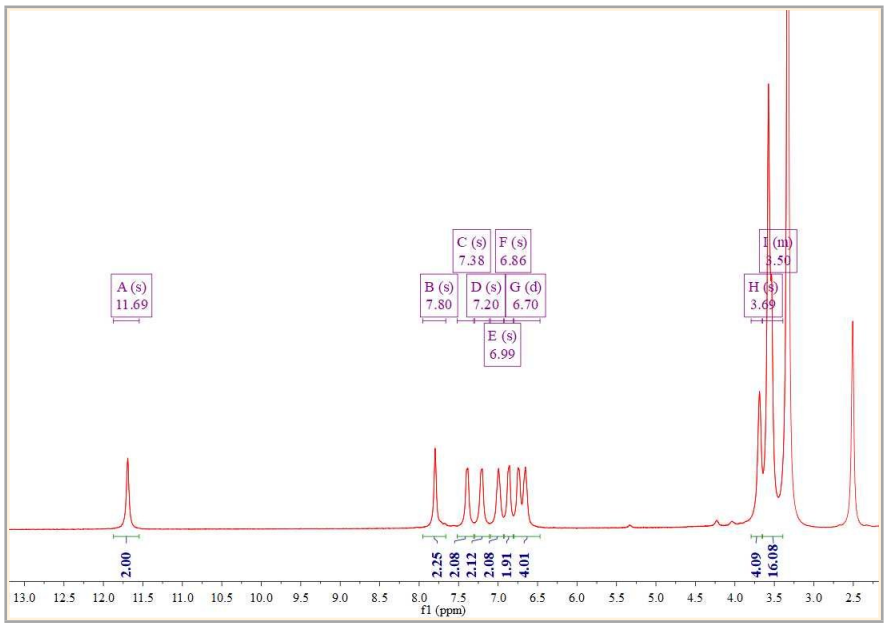

Fig. S19 ^{1}H NMR spectrum of ACE-BIM

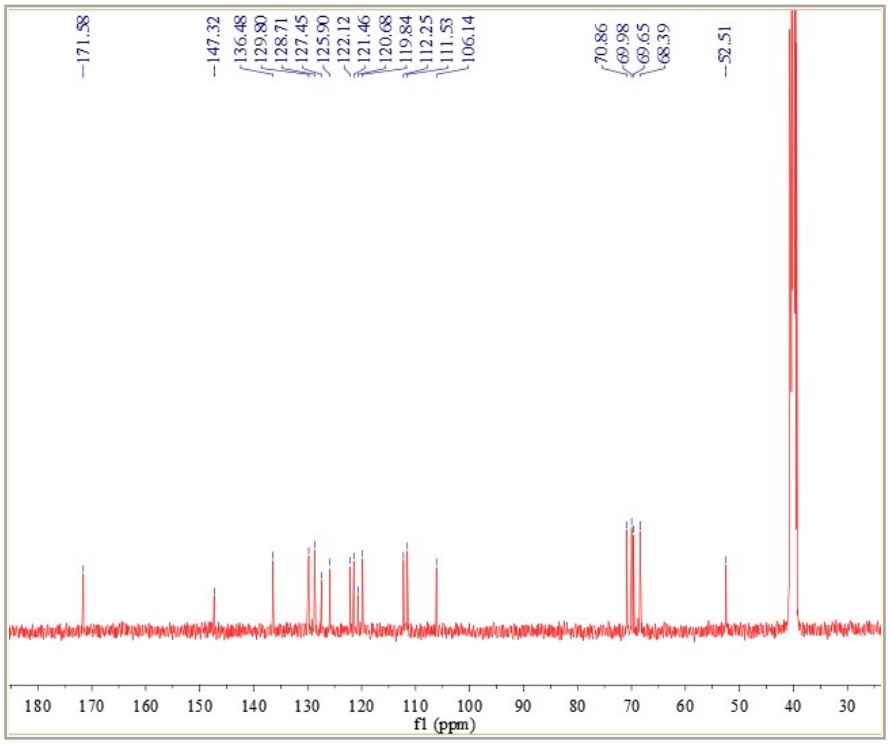

Fig. S20 ^{13}C NMR spectrum of ACE-BIM

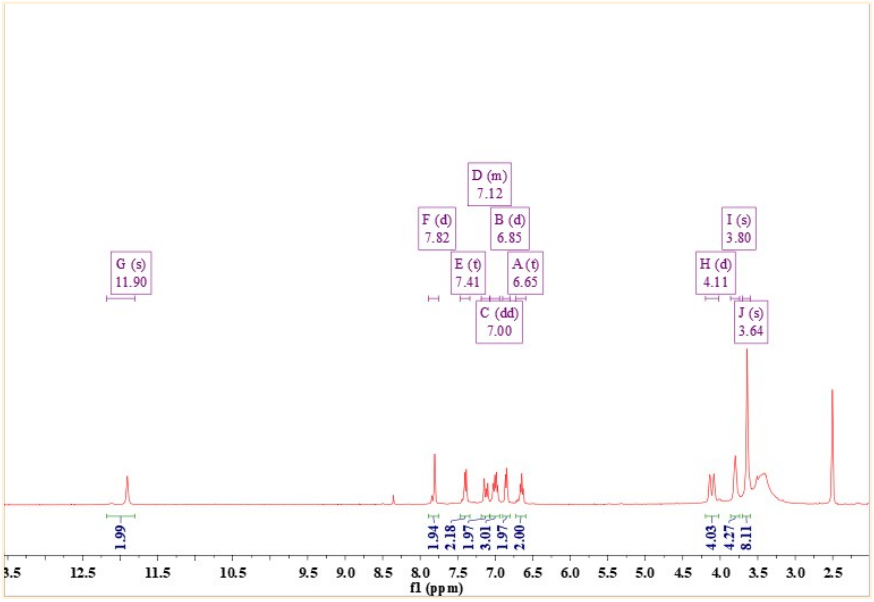

Fig. S21 ^{1}H NMR spectrum of BCE-BIM

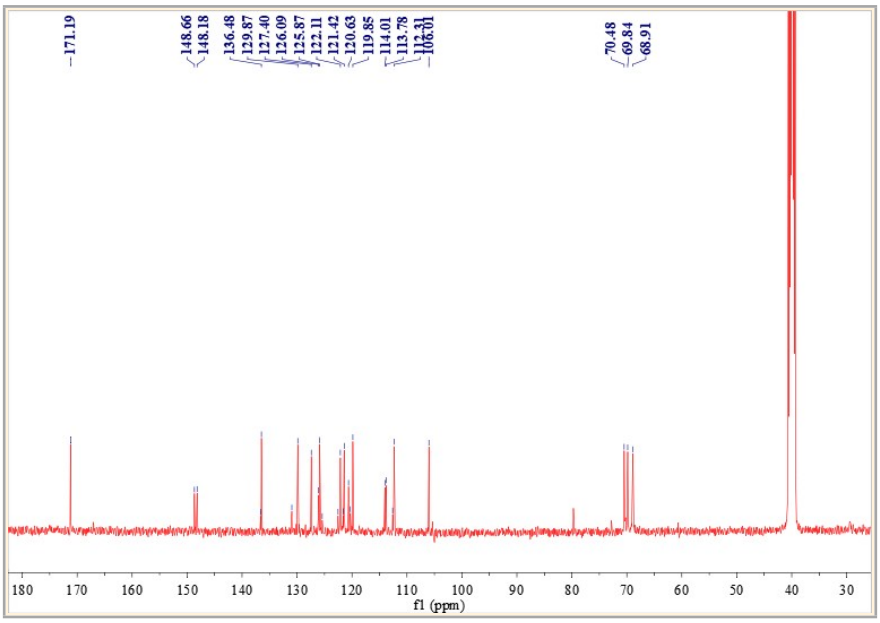

Fig. S22 ^{13}C NMR spectrum of BCE-BIM

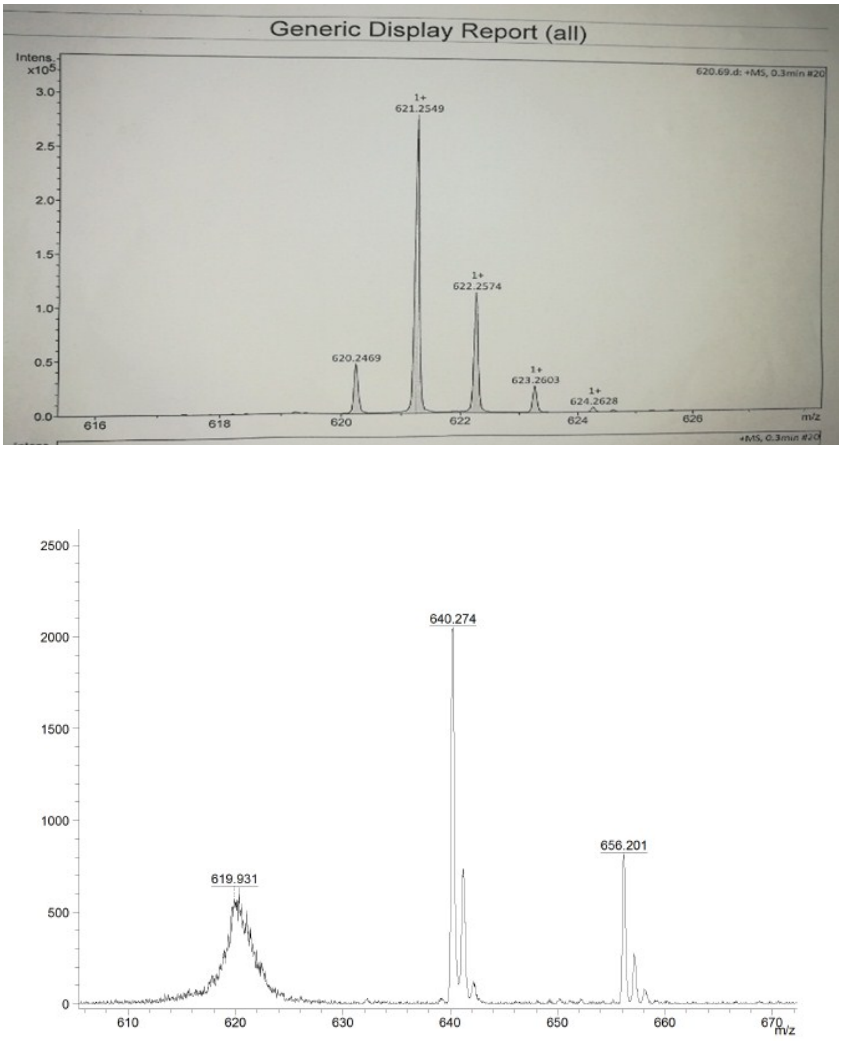

Fig. S23 MALDI-TOF MS of ACE-BIM (upper) and ACE-BIM-c (bottom).

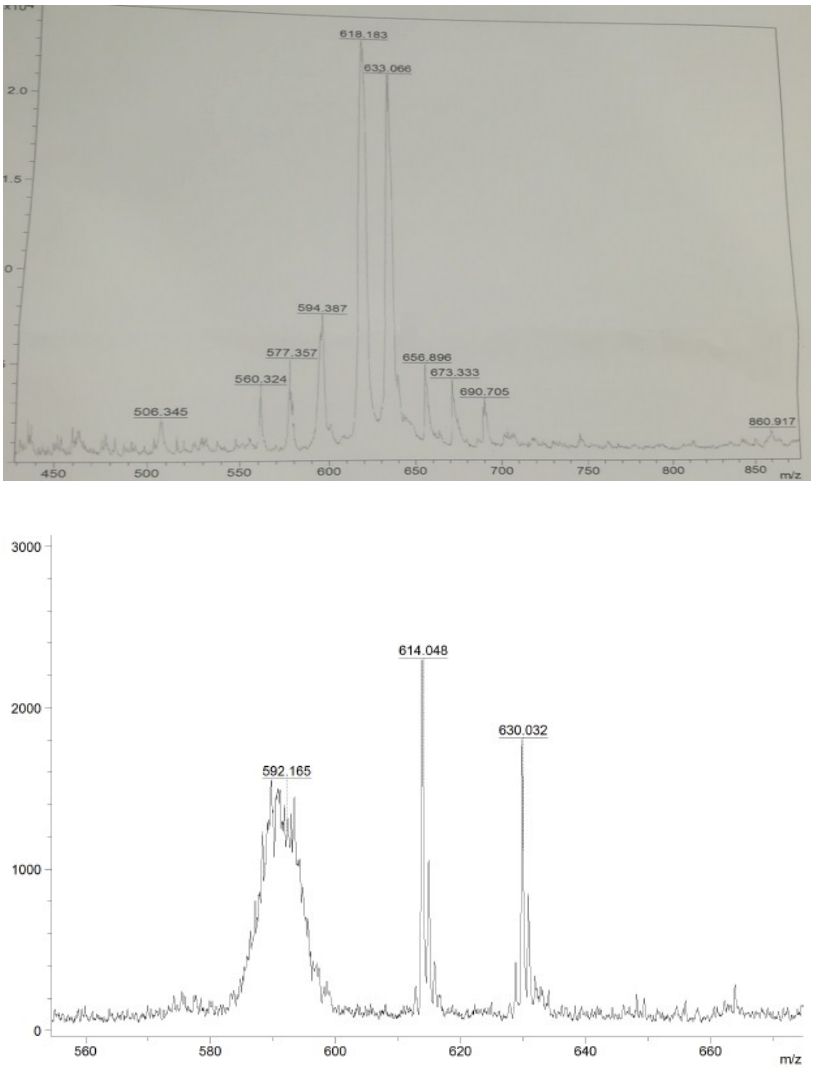

Fig. S24 MALDI-TOF MS of BCE-BIM (upper) and BCE-BIM-c (bottom).